NASA TN D-65

TECHNICAL NOTE

D-65

PROPELLANT VAPORIZATION AS A CRITERION FOR ROCKET-ENGINE DESIGN; EXPERIMENTAL EFFECT OF CHAMBER DIAMETER ON LIQUID OXYGEN - HEPTANE PERFORMANCE

By Marcus F. Heidmann

Lewis Research Center
Cleveland, Ohio

NATIONAL AERONAUTICS AND SPACE ADMINISTRATION

WASHINGTON September 1959

NATIONAL AERONAUTICS AND SPACE ADMINISTRATION

TECHNICAL NOTE D-65

PROPELLANT VAPORIZATION AS A CRITERION FOR ROCKET-ENGINE DESIGN; EXPERIMENTAL EFFECT OF CHAMBER DIAMETER ON LIQUID OXYGEN - HEPTANE PERFORMANCE

By Marcus F. Heidmann

SUMMARY

The effect of combustor gas velocity on the performance of a pair of impinging heptane jets reacting in a highly atomized oxygen atmosphere was evaluated in a nominal 200-pound-thrust combustor. Contraction-ratio changes resulting from variations in chamber diameter were used to vary combustor gas velocity. Characteristic velocity as a function of chamber length was obtained for four diameters corresponding to contraction ratios of 2.17, 3.60, 6.40, and 11.0. The study was made with a single injector and at one propellant-flow condition.

In combustors less than 10 inches long, highest performance was obtained with the large-contraction-ratio combustors. In chambers greater than 10 inches long, the reverse trend of performance with contraction ratio was observed. A direct comparison of this experimental effect and the analytical effect presented in the literature showed that the experimental reversal occurred in a longer chamber and at higher performance than predicted. In the high-performance region the increase in performance with a decrease in contraction ratio was similar in magnitude to that indicated analytically.

INTRODUCTION

Experimental and analytical studies of propellant vaporization in rocket combustors are a continuing effort at the Lewis Research Center (refs. 1 to 6). These studies are based on the hypothesis that propellant vaporization is the controlling factor in rocket-engine combustion. On the basis of this hypothesis, the effects of various combustor parameters on performance can be calculated, and specific interpretations of experimental data can be obtained. This paper presents a study of the experimental effect of combustor diameter on performance and an analysis of this effect on the basis of propellant vaporization.

Chamber diameter was varied, while the exhaust nozzle, injector, and propellant flow were maintained as essentially fixed. Combustor contraction ratio was varied by the changes in diameter. With ideal gas flow, combustor gas velocity is approximately inversely proportional to contraction ratio. The study of diameter changes, therefore, should test the effect of gas velocity on liquid-propellant combustion.

Analytical studies in references 1 to 3 report the calculated effect of combustor gas velocity on propellant vaporization. The gas-velocity index used was the final gas velocity attained in a cylindrical combustor with complete combustion. Such final gas velocities represent specific-contraction-ratio combustors. It was concluded in the analytical study of reference 3 that the chamber lengths needed to obtain equal performance vary inversely with the 0.4 power of final gas velocity; this was a gross effect weighted to a condition approaching complete vaporization. These analytical results imply that the small-diameter chambers produce higher performance than large-diameter chambers of equal length.

Liquid oxygen and heptane were used as propellants with an injector that produced more highly atomized oxygen than heptane. The study was intended to investigate heptane vaporization specifically in order to simulate the analytical model.

APPARATUS AND PROCEDURE

Combustor

The combustor was designed for a nominal thrust of 200 pounds at a chamber pressure of 300 pounds per square inch with liquid oxygen and heptane as propellants. A convergent nozzle with a throat diameter of 0.791 inch (shown in fig. 1) was used for all tests. Chamber diameters of 1.165, 1.50, 2.0, and 2.60 inches, giving contraction ratios of 2.17, 3.60, 6.40, and 11.0, respectively, were used. Cylindrical chamber lengths of 2 to 16 inches were tested. Nozzle convergence was not altered for chamber diameter; this resulted in abrupt cross-sectional area changes. The uncooled nozzle, cylindrical chamber, and injector were separable units.

Injector

The injector used in the study, shown in figure 2, consisted of two impinging heptane jets, 0.089 inch in diameter, with a 90° impingement angle. The flat fuel spray was midway between, and parallel with, two parallel rows of axial oxidant jets. A total of 24 oxygen jets, 0.032 inch in diameter, was used. The injector was intended to produce a

well-defined, reproducible heptane spray in an atmosphere of highly atomized liquid oxygen. Fuel tubes having a large length-to-diameter ratio were used to ensure solid stream impingement. A similar injector was used in experimental studies reported in references 5 and 6.

Test Facilities

A pressurized-tank propellant-flow system identical to that of reference 7 was used. Liquid-oxygen temperature was stabilized at -320° F by a liquid-nitrogen bath, which extended up to the propellant control valve and included the flowmeter and the propellant tank. Spark ignition was used for all tests.

Performance Measurements

Characteristic exhaust velocity c^* was used to measure engine performance. Chamber pressure was measured at the injector face with a direct-recording Bourdon instrument and with a strain-gage pressure transducer. Propellant-flow-rate measurements were made with rotating-vane-type flowmeters. Instrument calibrations indicated an accuracy within ±2 percent for c^*. Reproducilility of data was generally within ±1 percent.

The c^* evaluations are reported as a percentage of the theoretical performance at the operating mixture ratio (c^* efficiency). Theoretical equilibrium performance for heptane and oxygen at 300 pounds per square inch was used (ref. 7, fig. 13).

Procedure

Combustor tests of approximately 3-second duration were made at a desired total propellant-flow rate of 0.9 pound per second and a mixture ratio of 2.4. A range of mixture ratios was covered with several combustor assemblies in order to test performance sensitivity to this parameter.

EXPERIMENTAL RESULTS

The experimental characteristic velocity (c^*) data are shown in figure 3 as a function of mixture ratio for the various chamber lengths used for each contraction ratio. These data are also presented in table I.

A single performance value for each combustor configuration is used in the subsequent analysis. For this purpose, the value at a mixture ratio of 2.4 was obtained from the curves in figure 3. The values selected are shown in table II.

The observed c^* is a performance value uncorrected for momentum pressure losses. The measurement of chamber pressure at the injector face resulted in an observed pressure that was higher than the actual total pressure of the exhaust gases. This pressure loss is a function of contraction ratio, with the largest loss occurring in small-contraction-ratio combustors. The momentum-pressure-loss correction is described in reference 8 and other sources; equations (3-13) and (3-41) of reference 8 were used to make this correction. Table II shows the momentum-loss corrections.

Heat losses to the uncooled combustors gave an observed c^* that was lower than actual. Since heat transfer was not measured, a correction can only be approximated. The approximation used was:

$$\frac{c^*_{corr}}{c^*_{obs}} = \sqrt{\frac{H_{corr}}{H_{obs}}} = \sqrt{1 + \frac{\Delta H}{H_{obs}}} \qquad (1)$$

where c^*_{corr} and c^*_{obs} are the corrected and experimentally observed c^*, H_{corr} and H_{obs} are the total enthalpy before and after heat loss, and ΔH is the enthalpy loss due to heat transfer.

The enthalpy loss ΔH was assumed proportional to the product of chamber surface area, mass-flow rate per unit area, and the square of c^*_{obs}. The value of c^* squared in this instance was used as an index of the temperature differential between gas and wall, with the wall temperature assumed to be negligible. The enthalpy after heat loss H_{obs} was assumed proportional to the product of total weight flow and the square of c^*_{obs}. The value of c^* squared in this case was used as an index of the total temperature.

The heat-transfer correction was computed with the aid of the following data. In reference 6, heat-transfer measurements were made with an injector identical to that of this study. The enthalpy loss per unit area of a 2-inch diameter chamber was 1.18 Btu per second per square inch for a c^* of 4500 feet per second and a total weight flow of 0.93 pound per second of heptane and oxygen. For total enthalpy, a heat of combustion of 20,000 Btu per pound for heptane was assumed. At a mixture ratio of 2.4, the enthalpy rise for complete combustion (c^* of 5940 ft/sec) would be about 4000 Btu per pound of propellant. If the heat loss in the short nozzles used in these studies is considered to be negligible, the heat-transfer correction becomes

$$\frac{c^*_{corr}}{c^*_{obs}} = \sqrt{1 + 6.95 \times 10^{-3} \frac{l_{cyl}}{d_c}} \qquad (2)$$

where l_{cyl} and d_c are the cylindrical length and diameter of the combustor. A tabulation of these corrections is shown in table II.

Corrected values of c^* are shown in table II as a percentage of the theoretical value (c^* efficiency). Figure 4 also shows values of c^* efficiency at a mixture ratio of 2.4 corrected for heat-transfer and momentum loss as a function of cylindrical chamber length for each contraction ratio. These corrected values are used in the subsequent discussion.

ANALYSIS AND DISCUSSION

General Observations

Figure 4 shows that, in chambers less than 10 inches long, highest performance at a mixture ratio of 2.4 was obtained with large-contraction-ratio combustors. Beyond 10 inches, highest performance was obtained with small-contraction-ratio combustors. A high gas velocity, therefore, improved the combustion in long chambers and was detrimental to combustion in short chambers. This inversion of the effect of contraction ratio and gas velocity occurred at a c^* of 80 to 84 percent of theoretical. The high-performance region could not be fully explored because of the onset of combustion instability and the attendant burnout problems in long chambers.

A correlation of performance with chamber volume is implied by the performance characteristic in chambers less than 10 inches long. Performance as a function of characteristic length L^* (cylindrical volume/nozzle throat area) is shown in figure 5. Performance does not correlate with L^*; higher performance was obtained in small-, rather than large-, contraction-ratio combustors of equivalent L^*.

The performance trends shown in figure 4 are similar to analytical results based on drop vaporization. The effect of contraction ratio (final gas velocity) was computed for a single drop in reference 1 and for a distribution of drop sizes in reference 2. In both cases a reduction in contraction ratio decreased the length of combustor needed for complete vaporization. This effect, however, was not constant throughout the vaporization period. During the initial vaporization phase, as shown in reference 1, an inverse effect of contraction ratio was obtained. Inversion occurs in the region where combustion gas velocity begins to exceed drop velocity. This analytical result is similar to

the experimental effect shown in figure 4, where efficiency improves with an increase in contraction ratio in the low-efficiency region and the inverse effect becomes evident as efficiency increases.

Analytical Effect

A more complete analysis of the experimental results can be made by using the analytical results from reference 2 as a basis for comparison: The calculated results are for a heptane spray with a mean deviation of 2.3, which approximates the drop-size distribution obtained with impinging jets. Mass vaporized was correlated with an effective-length factor. The effective length is an adjustment of combustor length for typical combustor parameters. In the process of obtaining this correlation, the independent effect of contraction ratio (final gas velocity), as well as other combustor parameters, was computed. Figure 6 shows the independent effect for contraction ratios of 2.17, 3.60, 6.40, and 11.0. This specific analytical result is used in interpreting the experimental data.

Normalization of Data

The independent effect of contraction ratio shown in figure 6 is for a chamber pressure of 300 pounds per square inch, initial drop temperature of 500° R, initial drop velocity of 100 feet per second, and a mass mean drop radius of 0.003 inch. The experimental data were normalized to these conditions, with all mean performance values assumed to be for a total flow rate of 0.9 pound per second. Based on correlation factors reported in reference 3, the following expression for normalized length was used:

Normalized combustor length =

$$L_c \left[\left(\frac{P_c}{300} \right)^{0.66} \left(\frac{100}{v_0} \right)^{0.75} \left(\frac{0.003}{r} \right)^{1.45} \left(\frac{1 - 0.515}{1 - T_r} \right)^{0.4} \right] \tag{3}$$

$$L_c = \left[l_{cyl} + l_n \left(\frac{\bar{p}_n}{P_c} \right)^{0.66} \left(\frac{\bar{U}_n}{\bar{U}_c} \right)^{0.4} \right] \tag{4}$$

where

L_c combustor length adjusted for nozzle effect, in.

l_{cyl} cylindrical chamber length, in.

l_n exhaust nozzle length, in.

P_c total pressure at nozzle inlet, lb/sq in.

$\bar{P}_n$ average nozzle static pressure, lb/sq in.

T_r ratio of initial to critical temperature for heptane (critical temp., 969° R)

r mass mean drop radius, in.

U_c final combustor gas velocity, ft/sec

$\bar{U}_n$ average nozzle gas velocity, ft/sec

v_0 initial drop velocity, ft/sec

This expression was evaluated in the following manner.

Chamber pressure. - With constant total-weight-flow operations the chamber pressure varied directly with c* efficiency. The data were normalized to 300 pounds per square inch by multiplying combustor length by the factor $(P_c/300)^{0.66}$ (eq. 3).

Initial drop temperature. - No correction for initial temperature was made. Injection temperatures were very nearly equal to 500° R, the reference condition.

Initial drop velocity. - The injection velocity for the experimental data being analyzed was 65 feet per second. For a 90° impingement of the jets a resultant velocity of 46 feet per second is obtained and is assumed to be the initial drop velocity. The combustor length was increased by the factor $(100/46)^{0.75}$ in order to normalize the data to 100 feet per second.

Drop radius. - Drop-size data for jets impinging within a combustor are not available, and a drop size had to be assumed. A mass mean drop radius of 0.0107 inch was assumed, and chamber length was reduced by the factor $(0.003/0.0107)^{0.4}$ for all conditions. As a check on this assumption, the drop size was compared with drop-size measurements for impinging jets in various gas-velocity environments reported in reference 9. For the jet conditions used in these tests, reference 9 data indicate that a mean drop radius of 0.0107 inch is produced by a velocity difference of 10 feet per second between gas and jet; this indicates a gas velocity of either 55 or 75 feet per second in the region of spray formation. Such gas velocities appear reasonable for these tests.

Nozzle length and conditions. - A combustor length equal to the cylindrical length plus an adjusted nozzle length was used. Actual nozzle length was 1 inch in all tests; the length was modified, however, to account for the fact that velocity was higher and pressure was lower than in the cylindrical chamber. The following adjustment was used:

$$l_n\left(\frac{\bar{p}_n}{P_c}\right)^{0.66}\left(\frac{\bar{U}_n}{U_c}\right)^{0.4}$$

where $\bar{p}_n/P_c$ was the ratio of average nozzle pressure to chamber pressure, and $\bar{U}_n/U_c$ was the ratio of average nozzle velocity to final chamber velocity. For a critical-flow nozzle, the throat pressure equals about one-half the chamber pressure, which gives a $\bar{p}_n/P_c$ equal to 0.75. The ratio of nozzle exit to entrance velocity is approximately equal to $\frac{3}{2} A_c/A_t$ (contraction ratio). Therefore, $\bar{U}_n/U_c$ would equal $1/2\ (1 + \frac{3}{2} A_c/A_t)$. Adjusted nozzle lengths based on these assumptions were added to cylindrical chamber length to obtain a total combustor length as indicated in table II.

Propellant vaporized. - The fraction of propellant vaporized was computed from c^* efficiency, with propellant vaporization assumed to be the single process controlling combustion. The fraction of heptane vaporized was computed by the method described in reference 4. Complete oxygen vaporization was assumed for all conditions.

Comparison of Analytical and Experimental Data

The normalized experimental data are shown in figure 7, where the fraction of heptane vaporized is presented as a function of normalized length. When figure 7 is compared directly with the analytical results in figure 6, the experimental length needed to vaporize a given fraction of heptane agrees with the analytical result. Some detailed differences in analytical and experimental results, however, are evident: The inverse effect of contraction ratio is predicted to occur at a length of 1 inch with 30 percent of the heptane vaporized; this condition occurs experimentally at a length of about 3 inches with 60 percent of the heptane vaporized.

When the data of figure 7 are extrapolated, the effect of contraction ratio on propellant vaporized agrees qualitatively with analysis. The extrapolated curves at 90 percent heptane vaporized show that length varies inversely by the factor $(A_c/A_t)^{0.55}$. Analytically the factor was $(A_c/A_t)^{0.4}$. Within the precision of the extrapolation, quantitative

agreement between the analytical and experimental effect of contraction ratio may be assumed. Figure 8 shows the data normalized to a contraction ratio of 3.15. Chamber length was adjusted by the factor $\left(\frac{3.15}{A_c/A_t}\right)^{0.4}$ for this normalization. The shaded area in figure 8 indicates the degree of correlation obtained with analytical results. A comparatively poor correlation of the experimental results in the initial phases of vaporization is evident; however, the correlation improves in approaching the region where 70 percent or more of the heptane is vaporized.

Limitations of Experimental Tests

Differences between conditions of the experimental tests and the analytical model may have contributed to a lack of complete correlation of results. Although these differences cannot be resolved from the data in this study, the following possibilities exist:

(1) Median drop size may change when combustor parameters vary. Interpreting the data on this basis would require a decrease in drop size with an increase in contraction ratio, with the effect diminishing as chamber length increases. If spray breakup occurs when spray velocity is higher than gas velocity, the velocity difference would increase with contraction ratio and thereby reduce drop size. This effect would diminish as chamber length increases. An analysis of gas velocity similar to that made in reference 6 indicates that near the injector the gas-velocity changes with contraction ratio are less severe in long, rather than short, chambers. Additional combustion data and an extension of atomization theory in accelerating gas media are needed, however, for an evaluation of this effect.

(2) Spray characteristics may change because of wall interference when combustor diameter varies. Large diameters may favor spray development and vaporization and thus counteract the effect of contraction ratio on performance. The independent effect of contraction ratio should not include the effect of wall interference.

(3) Exhaust nozzle effects, predicted on the basis of average velocity and pressure conditions, showed an increase in effective nozzle length with an increase in contraction ratio (table II). A larger increase in effective length is probable if rate of change in velocity and pressure are considered. In a constant-length nozzle, as was used in these tests, both velocity and pressure change more rapidly as contraction ratio is increased. These sudden changes may cause drop shattering and contribute to the high performance of large-contraction-ratio combustors. The effect would be most severe in short chambers when large heptane drops enter the nozzle. Additional information on the dynamics of drops in convergent nozzles is needed to resolve this effect.

SUMMARY OF RESULTS

Characteristic velocity as a function of chamber length was obtained for four chamber diameters corresponding to contraction ratios of 2.17, 3.60, 6.40, and 11.0. The following results were obtained:

1. In combustors less than 10 inches long, highest performance was obtained with large contraction ratios (low combustor gas velocity). High performance with small contraction ratio (high combustor gas velocity) developed in combustors greater than 10 inches long. The inversion occurred at a characteristic exhaust velocity of 80 to 84 percent of theoretical.

2. An inversion in the effect of contraction ratio on performance is in agreement with analytical results based on drop vaporization theory. The experimental inversion occurred at a longer length and higher performance than that predicted.

3. In the high-performance region, the increase in performance with a decrease in contraction ratio was similar in magnitude to that predicted on the basis of drop vaporization.

Lewis Research Center
National Aeronautics and Space Administration
Cleveland, Ohio, June 25, 1959

REFERENCES

1. Priem, Richard J.: Propellant Vaporization as a Criterion for Rocket-Engine Design; Calculations of Chamber Length to Vaporize a Single n-Heptane Drop. NACA TN 3985, 1957.

2. Priem, Richard J.: Propellant Vaporization as a Criterion for Rocket-Engine Design; Calculations Using Various Log-Probability Distributions of Heptane Drop. NACA TN 4098, 1957.

3. Priem, Richard J.: Propellant Vaporization as a Criterion for Rocket-Engine Design; Calculations of Chamber Length to Vaporize Various Propellants. NACA TN 3883, 1958.

4. Heidmann, Marcus F., and Priem, Richard J.: Propellant Vaporization as a Criterion for Rocket Engine Design; Relation Between Percentage of Propellant Vaporized and Engine Performance. NACA TN 4219, 1958.

5. Heidmann, M. F.: Propellant Vaporization as a Criterion for Rocket-Engine Design; Experimental Effect of Fuel Temperature on Liquid-Oxygen - Heptane Performance. NACA RM E57E03, 1957.

6. Clark, Bruce J., Hersch, Martin, and Priem, Richard J.: Propellant Vaporization as a Criterion for Rocket-Engine Design; Experimental Performance, Vaporization, and Heat-Transfer Rates with Various Propellant Combinations. NASA MEMO 12-29-58E, 1959.

7. Heidmann, M. F., and Auble, C. M.: Injection Principles from Combustion Studies in a 200-Pound-Thrust Rocket Engine Using Liquid Oxygen and Heptane. NACA RM E55C22, 1955.

8. Sutton, George P.: Rocket Propulsion Elements. Second Ed., John Wiley & Sons, Inc., 1956.

9. Ingebo, Robert D.: Drop-Size Distributions for Impinging-Jet Breakup in Airstreams Simulating the Velocity Conditions in Rocket Combustors. NACA TN 4222, 1958.

TABLE I. - EXPERIMENTAL PERFORMANCE DATA

Run	Fuel flow, lb/sec	Oxidant flow, lb/sec	Total flow, lb/sec	Chamber pressure, lb/sq in.	Mixture ratio	Characteristic velocity, ft/sec	Run	Fuel flow, lb/sec	Oxidant flow, lb/sec	Total flow, lb/sec	Chamber pressure, lb/sq in.	Mixture ratio	Characteristic velocity, ft/sec
Diameter, 1.165 in.; contraction ratio, 2.17							Diameter, 1.50 in.; contraction ratio, 3.60						
Length, 2 in.													
17	0.290	0.675	0.965	160	2.33	2620	20	0.269	0.645	0.914	161.5	2.40	2790
18	.265	.635	.900	147	2.40	2580	21	.262	.650	.912	152.5	2.48	2640
19	.245	.647	.892	142	2.64	2520	22	.260	.633	.893	150.5	2.43	2660
Length, 4 in.													
48	0.266	0.635	0.901	198	2.39	3460	23	0.249	0.660	0.909	187	2.65	3250
49	.267	.633	.900	194	2.37	3400	24	.248	.640	.888	184	2.58	3270
50	.251	.640	.891	193.5	2.55	3430	25	.251	.628	.879	181	2.50	3260
51	.246	.630	.876	192	2.56	3460							
Length, 6 in.													
26	0.245	0.643	0.888	226	2.63	4020	30	0.238	0.610	0.848	209	2.56	3890
27	.252	.633	.885	226	2.51	4030	31	.253	.620	.873	215.5	2.45	3900
28	.258	.620	.878	226	2.40	4060	32	.251	.675	.926	229	2.69	3900
Length, 8 in.													
12	0.259	0.635	0.894	265	2.45	4680	13	0.349	0.566	0.915	249	1.62	4300
37	.248	.618	.866	259	2.49	4710	14	.378	.511	.889	239.5	1.35	4250
38	.258	.612	.870	255.5	2.37	4640	15	.221	.722	.943	251.5	3.26	4210
39	.260	.612	.872	260.5	2.35	4710	16	.283	.668	.951	258.5	2.36	4300
84	.251	.623	.874	256	2.48	4620	91	.249	.620	.869	245	2.49	4450
85	.323	.564	.887	254	1.74	4520	92	.322	.556	.878	244	1.73	4380
86	.185	.692	.877	252.5	3.74	4550	93	.190	.709	.899	242.5	3.73	4260
87	.403	.477	.880	243	1.18	4360	94	.407	.465	.872	236.5	1.14	4290
88	.218	.650	.868	257	2.98	4680	95	.227	.660	.887	241	2.91	4300
89	.357	.521	.878	250	1.46	4500	96	.357	.512	.869	239	1.43	4350
90	.277	.590	.867	257	2.13	4680	97	.277	.598	.875	243	2.16	4380
Length, 12 in.													
98	0.278	0.643	0.921	310	2.31	5320	33	0.258	0.652	0.910	293	2.53	5090
99	.262	.646	.908	302	2.47	5260	34	.267	.653	.920	292	2.44	5010
Diameter, 2.0 in.; contraction ratio, 6.40							Diameter, 2.62 in.; contraction ratio, 11.0						
Length, 2 in.													
							59	0.274	0.645	0.919	210	2.35	3610
							60	.259	.660	.919	212	2.54	3650
							61	.249	.657	.906	204	2.64	3560
							62	.262	.608	.870	196	2.32	3560
							75	.259	.593	.852	198	2.29	3680
							76	.256	.613	.869	199	2.39	3620
							77	.248	.635	.883	204	2.56	3650
							78	.257	.628	.885	203.5	2.44	3630
Length, 4 in.													
55	0.277	0.645	0.922	228.5	2.33	3920	51	0.200	0.568	0.768	212	2.84	4360
56	.273	.623	.896	226	2.28	3980	52	.239	.632	.871	238	2.65	4320
57	.262	.642	.904	227.5	2.45	3980	53	.245	.630	.875	241.5	2.57	4360
							54	.246	.623	.869	242.5	2.53	4410
Length, 6 in.													
							63	0.239	0.622	0.861	252	2.60	4660
							64	.248	.616	.864	254	2.48	4640
							65	.245	.620	.865	253	2.53	4620
							79	.259	.593	.852	247.5	2.29	4550
							80	.248	.650	.898	259.5	2.62	4570
							81	.242	.645	.887	255.5	2.67	4560
Length, 8 in.													
40	0.255	0.622	0.877	261.5	2.44	4710	44	0.246	0.627	0.873	260	2.55	4700
41	.248	.640	.888	258.5	2.58	4600	46	.262	.600	.862	258	2.29	4730
42	.249	.637	.886	257	2.56	4580	47	.235	.640	.875	262	2.72	4730
Length, 12 in.													
67	0.245	0.623	0.868	273.5	2.54	4970							
68	.249	.638	.887	276.5	2.56	4930							
69	.256	.635	.891	277.5	2.48	4920							
70	.259	.623	.882	276.5	2.41	4950							
Length, 16 in.													
71	0.245	0.642	0.887	286.5	2.62	5100							
72	.242	.626	.868	278.5	2.59	5070							
73	.246	.610	.856	275	2.48	5080							

TABLE II. - CORRECTION AND NORMALIZATION OF EXPERIMENTAL PERFORMANCE AT MIXTURE RATIO OF 2.4

Chamber diameter, in.	Contraction ratio	Chamber length, in.	Characteristic velocity, c^*, ft/sec	Momentum $\frac{c^*_{act}}{c^*_{meas}}$	Heat-transfer $\frac{c^*_{act}}{c^*_{meas}}$	Corrected c^*, ft/sec	Corrected c^* efficiency, percent	Length normalization[a]				Heptane, vaporized, percent of total	Length	
								Chamber pressure, $\left(\frac{P_c}{300}\right)^{0.66}$	Nozzle length, $l_n\left(\frac{\bar{p}}{P_c}\right)^{0.66}\left(\frac{\bar{U}}{U_c}\right)^{0.4}$	Combustor length (chamber + nozzle), in.	Normalized length, in.		Contraction ratio, $\left(\frac{3.15}{A_c/A_t}\right)^{0.4}$	Normalized length including effect of contraction ratio, in.
1.185	2.17	2	2570	0.963	1.007	2530	42.6	0.616	1.12	3.12	0.54	16.2	1.16	0.63
		4	3440	↓	1.012	3360	56.6	.742	↓	5.12	1.08	28.3	↓	1.25
		6	4040		1.017	3950	66.5	.825		7.12	1.66	39.4		1.93
		8	4680		1.023	4620	77.8	.916		9.12	2.36	55.3		2.74
		12	5290		1.034	5260	88.6	.998		13.12	3.71	73.2		4.30
1.50	3.60	2	2700	0.980	1.005	2660	44.8	0.636	1.32	3.32	0.60	18.0	0.95	0.57
		4	3260	↓	1.010	3230	54.4	.722	↓	5.32	1.09	26.2	↓	1.04
		6	3900		1.014	3880	65.4	.818		7.32	1.69	38.0		1.61
		8	4360		1.018	4350	73.3	.881		9.32	2.33	48.5		2.21
		12	5050		1.027	5080	85.7	.976		13.32	3.68	68.0		3.50
2.0	6.40	4	3970	0.991	1.007	3960	66.7	0.826	1.61	5.61	1.31	39.5	0.75	0.98
		8	4640	↓	1.014	4660	78.5	.921	↓	9.61	2.51	56.5	↓	1.88
		12	4940		1.020	5000	84.2	.965		13.61	3.72	65.7		2.79
		16	5090		1.027	5170	87.1	.986		17.61	4.92	70.5		3.69
2.62	11.0	2	3630	0.997	1.003	3630	61.1	0.782	1.97	3.97	0.88	32.9	0.61	0.54
		4	4360	↓	1.005	4370	73.6	.884	↓	5.97	1.49	48.8	↓	.91
		6	4620		1.008	4640	78.2	.919		7.97	2.07	56.0		1.26
		8	4730		1.010	4770	80.3	.935		9.97	2.64	59.5		1.61

[a]Initial drop temperature $\left(\frac{1 - 0.515}{1 - T_r}\right)^{0.4}$, 1.00; drop velocity $\left(\frac{100}{V_0}\right)^{0.75}$, 1.788; drop radius $\left(\frac{0.003}{r}\right)^{1.45}$, 0.158.

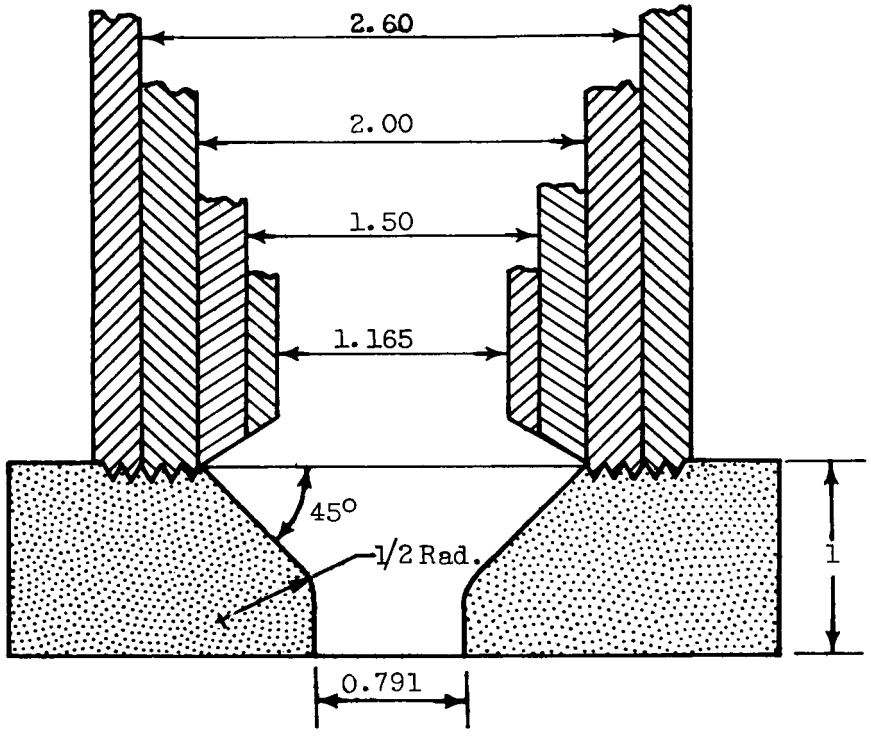

Figure 1. - Exhaust nozzle and entrance configuration.
(All dimensions in inches.)

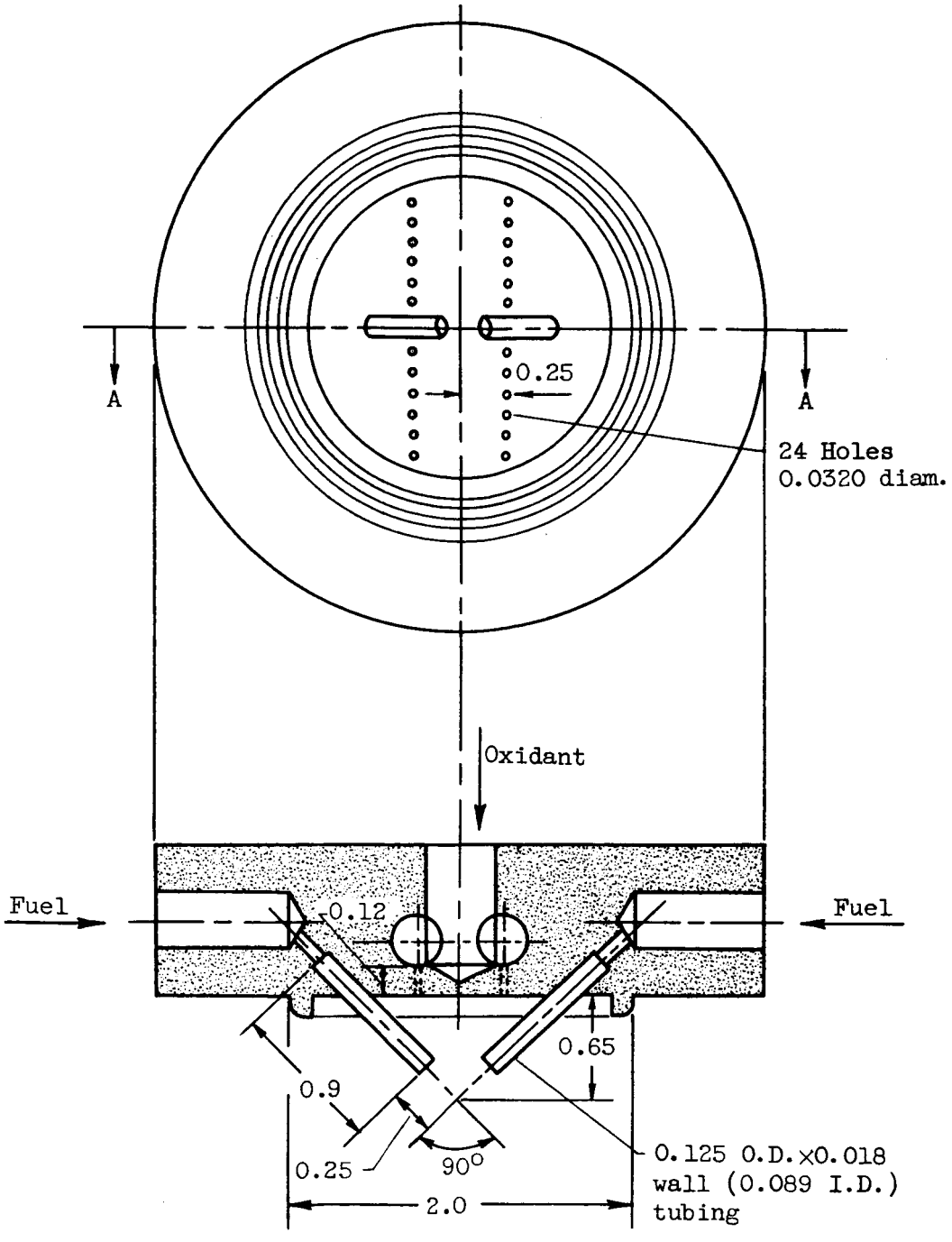

Section AA

Figure 2. - Injector design simulating impinging-jet fuel spray in a highly atomized oxidant atmosphere. (All dimensions in inches.)

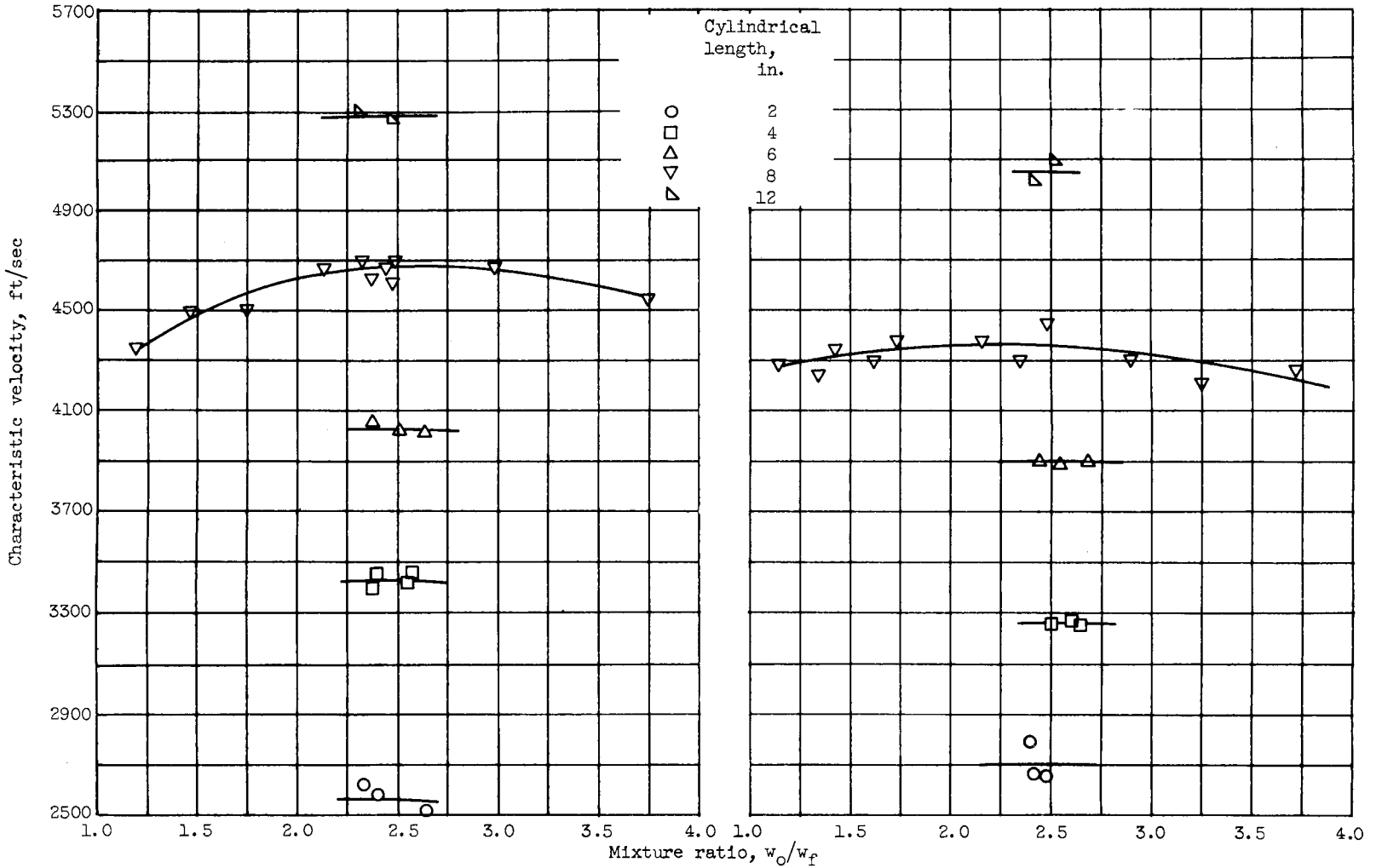

(a) Diameter, 1.165 inches; contraction ratio, 2.17.

(b) Diameter, 1.50 inches; contraction ratio, 3.60.

Figure 3. - Combustor performance.

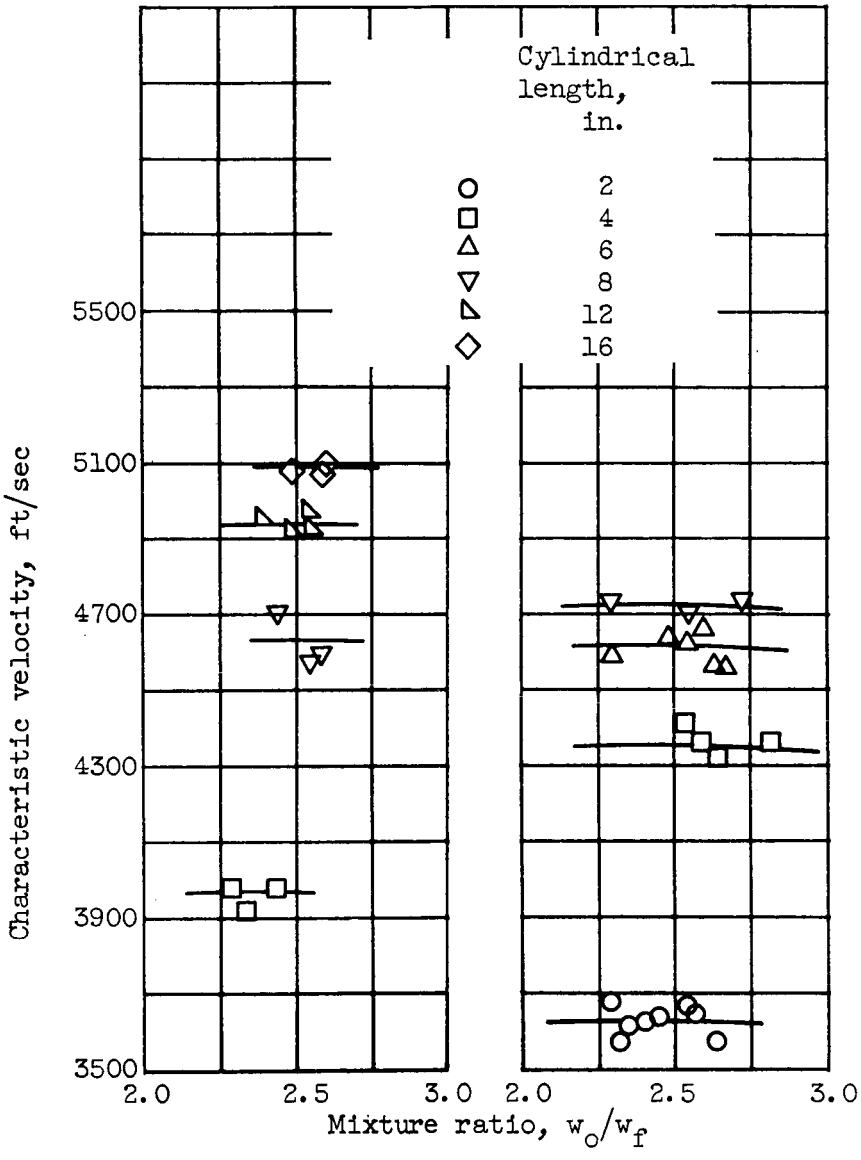

(c) Diameter, 2.0 inches; contraction ratio, 6.40.

(d) Diameter, 2.62 inches; contraction ratio, 11.0.

Figure 3. - Concluded. Combustor performance.

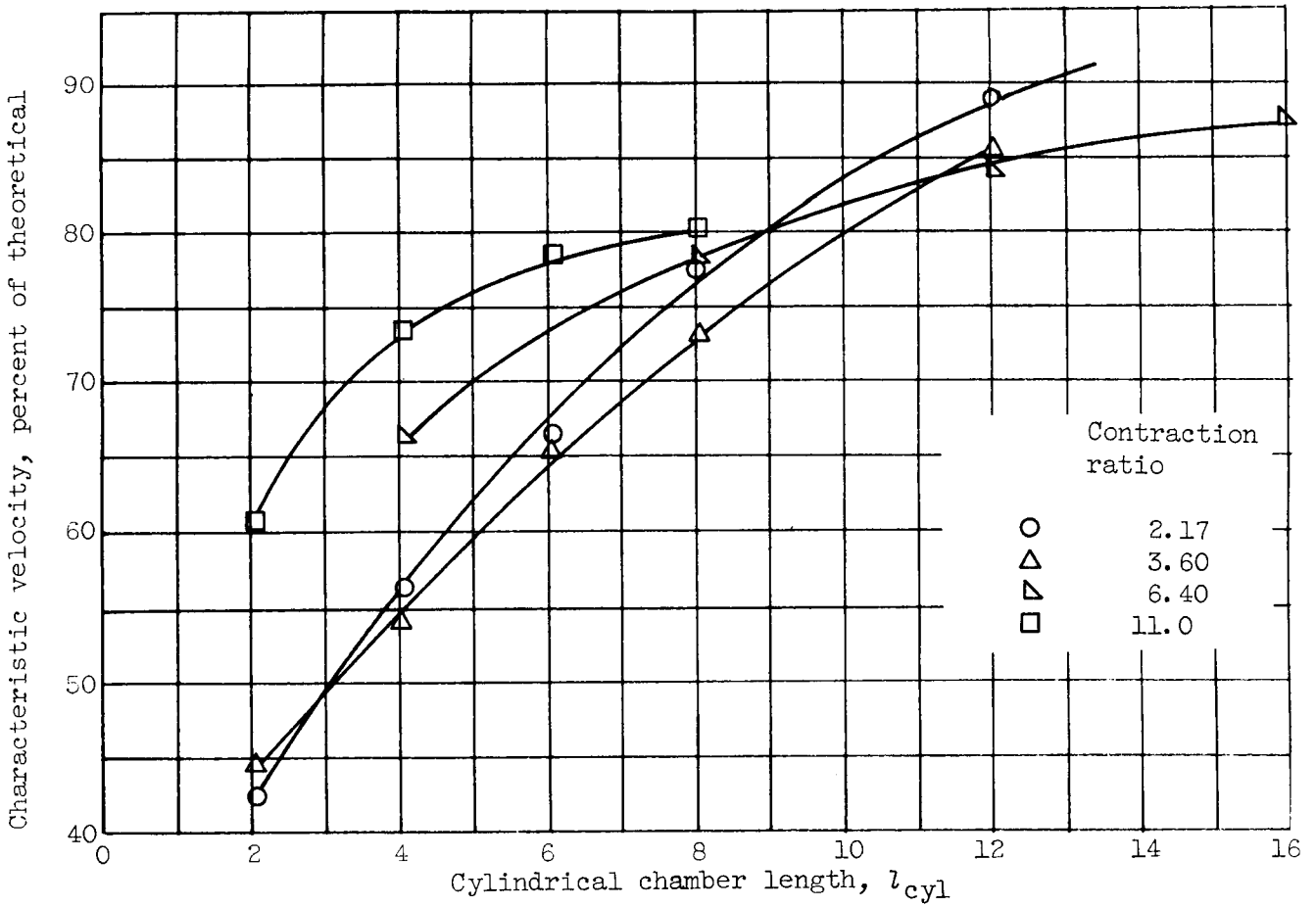

Figure 4. - Experimental performance at a mixture ratio of 2.4 corrected for heat-transfer and momentum loss.

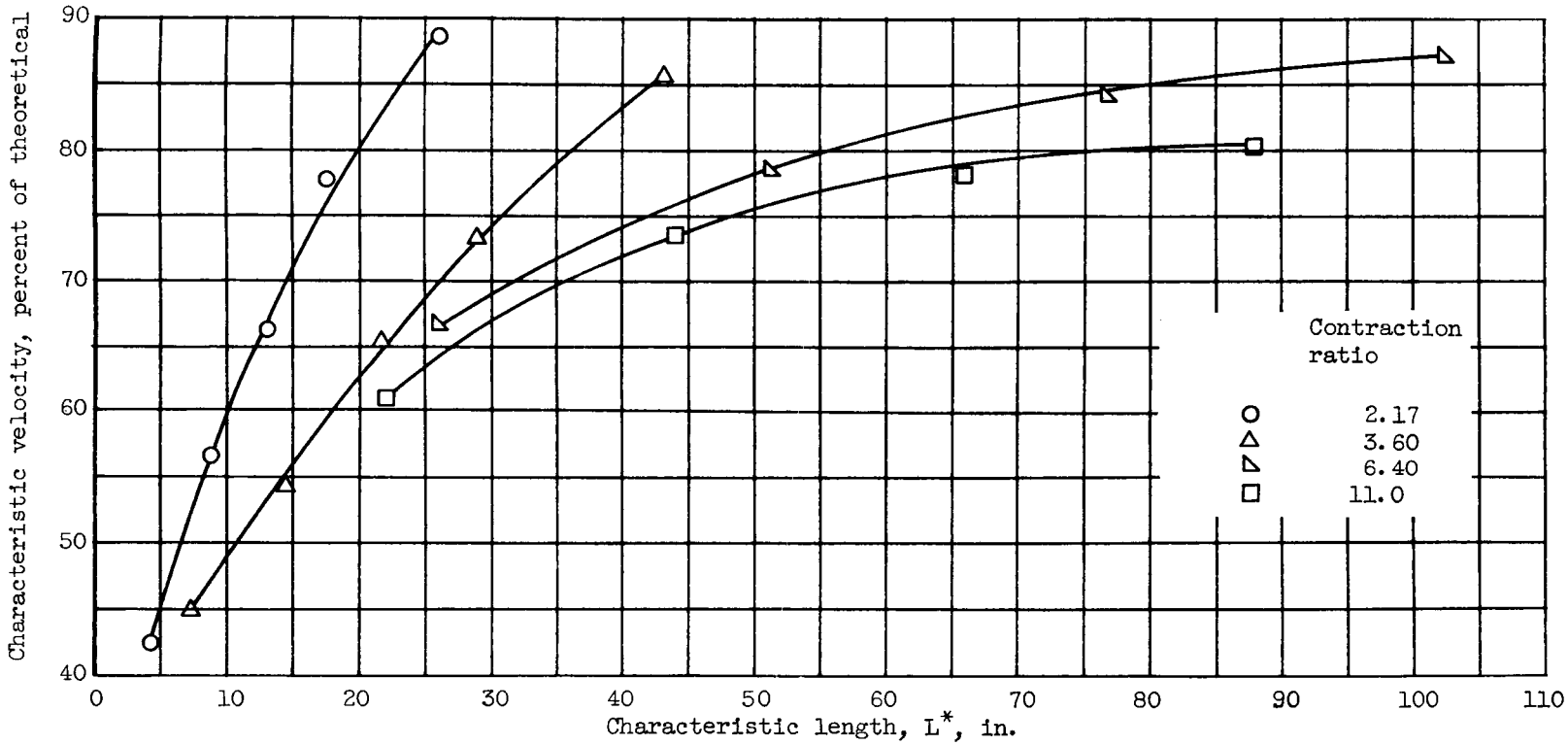

Figure 5. - Experimental performance as function of characteristic length.

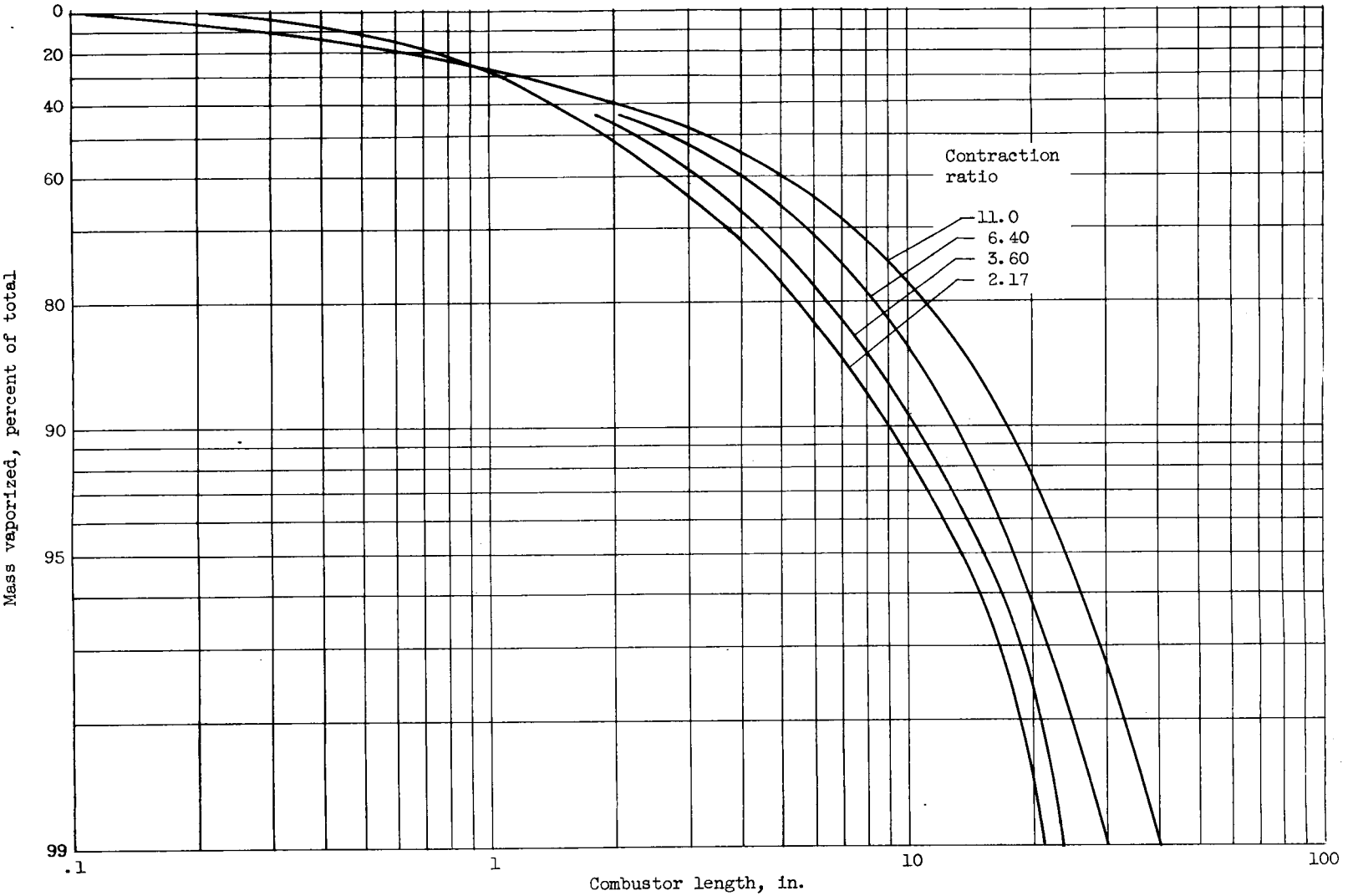

Figure 6. - Calculated combustor lengths for heptane at various contraction ratios. Pressure, 300 pounds per square inch; initial drop velocity, 100 feet per second; mean drop radius, 0.003 inch; initial drop temperature, 500° R.

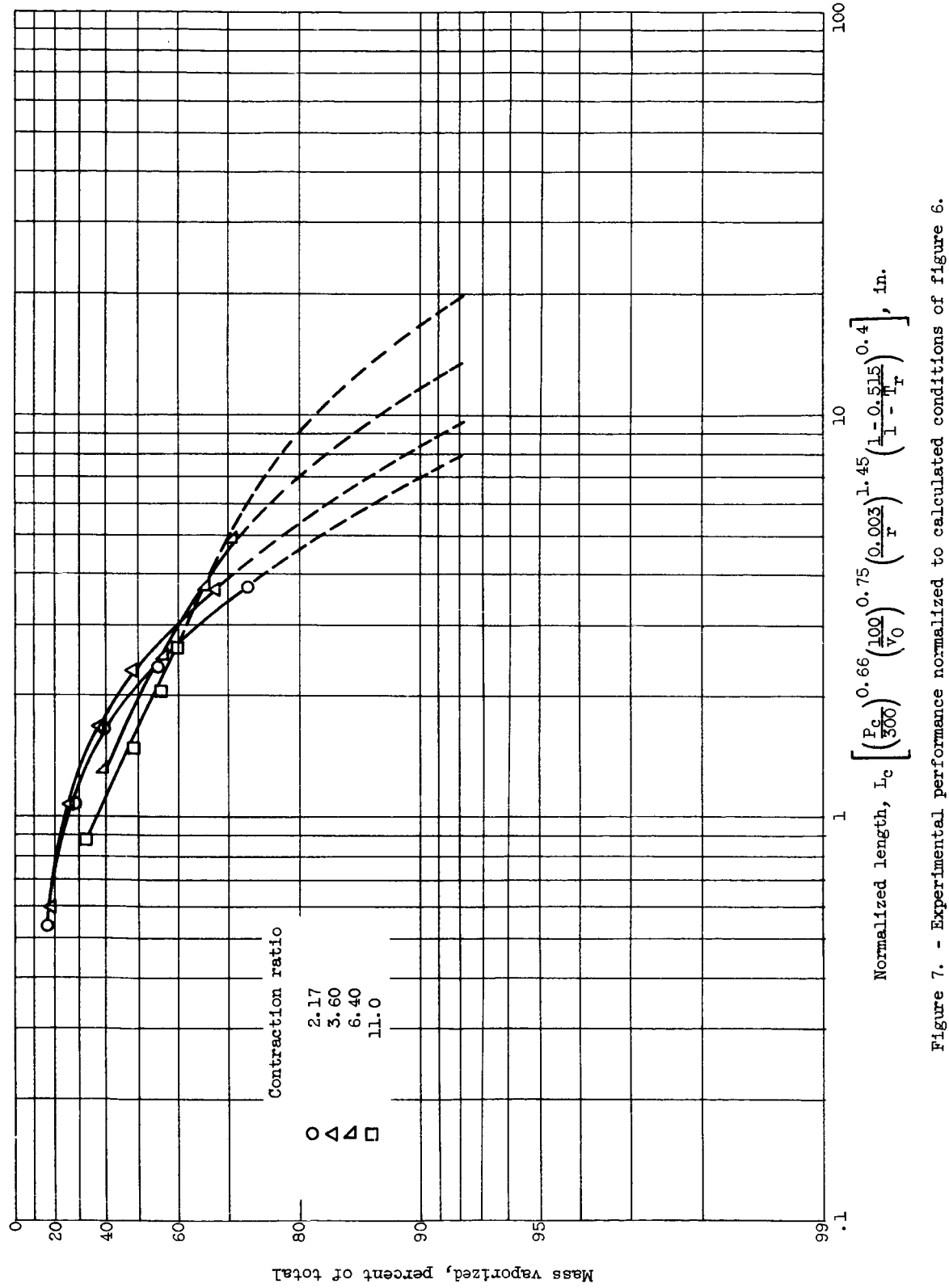

Figure 7. - Experimental performance normalized to calculated conditions of figure 6.

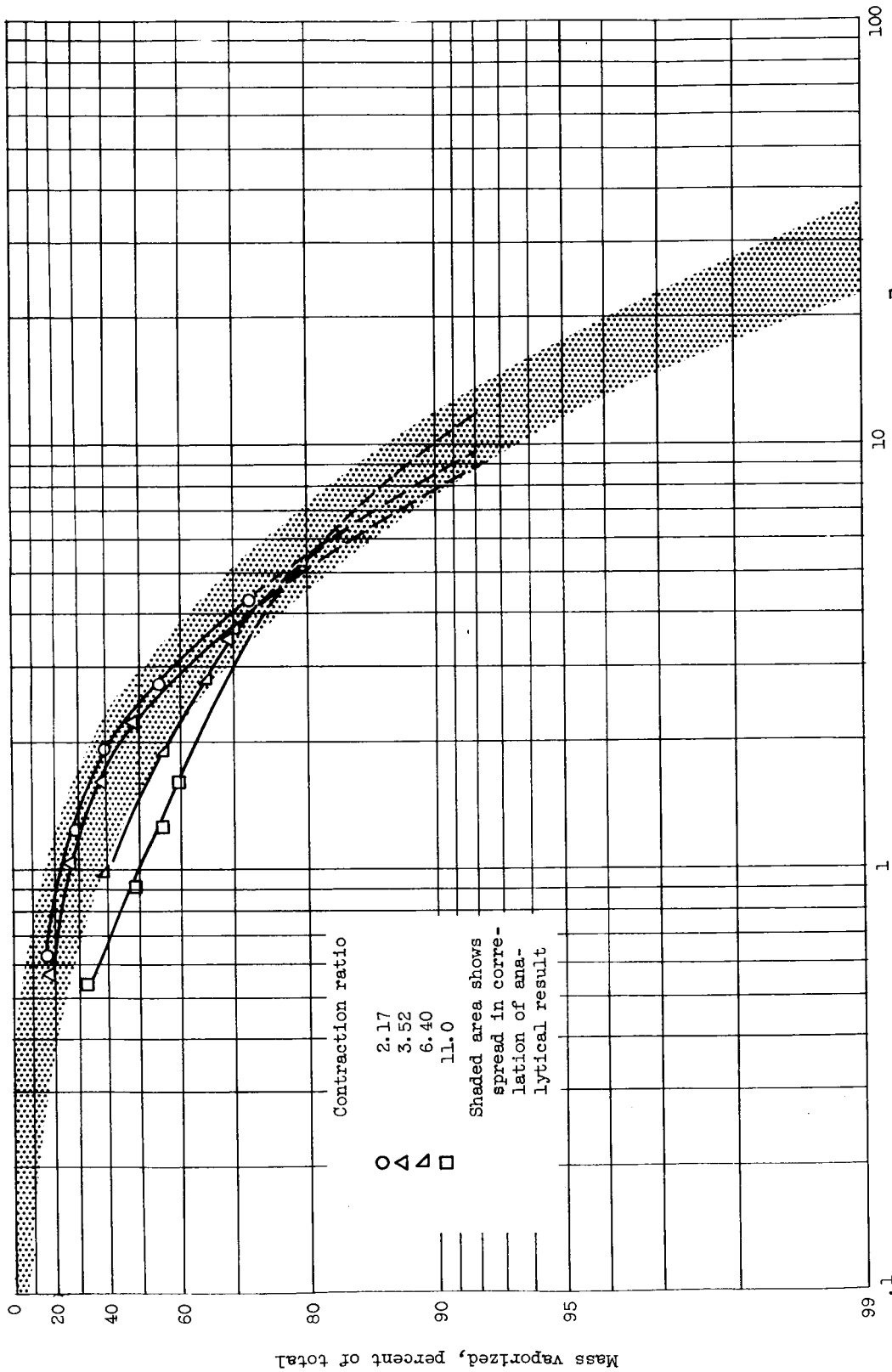

Figure 8. - Correlated experimental performance including effect of contraction ratio.